# ORIGINAL RESEARCH

Acvr1b Loss Increases Formation of Pancreatic Precancerous Lesions From Acinar and Ductal Cells of Origin

Kiyoshi Saeki,[1,2,3] Ian S. Wood,[4] Wei Chuan Kevin Wang,[4] Shilpa Patil,[4] Yanping Sun,[5] David F. Schaeffer,[6] Gloria H. Su,[1,2,3] and Janel L. Kopp[4]

[1]Department of Pathology and Cell Biology, Columbia University Irving Medical Center, New York, New York; [2]Herbert Irving Comprehensive Cancer Center, Columbia University Irving Medical Center, New York, New York; [3]Department of Otolaryngology and Head and Neck Surgery, Columbia University Irving Medical Center, New York, New York; [4]Department of Cellular and Physiological Sciences, Life Sciences Institute, University of British Columbia, Vancouver, Canada; [5]Oncology Precision Therapeutics and Imaging Core (OPTIC), Columbia University Medical Center, New York, New York; and [6]Department of Pathology and Laboratory Medicine, University of British Columbia, Vancouver, Canada
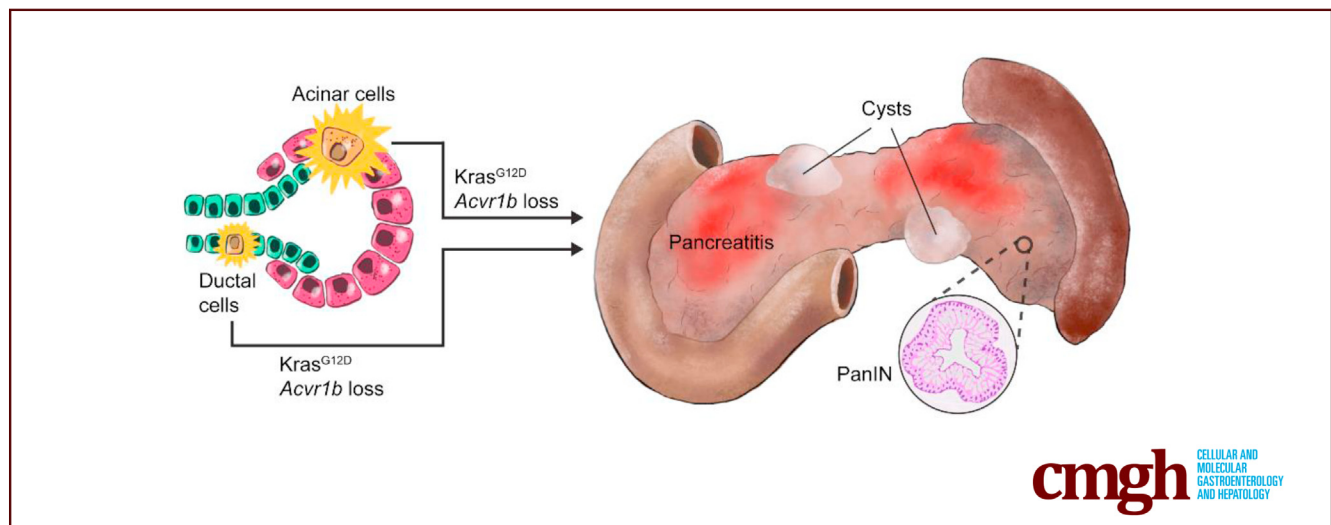
SUMMARY

Acvr1b loss in pancreatic Kras^{G12D}-expressing acinar or ductal cells promotes the development of precancerous lesions in the pancreas. These precancerous lesions get larger with time in the absence of *Acvr1b* and resemble intraductal papillary mucinous neoplasia.

BACKGROUND & AIMS: Pancreatic ductal adenocarcinoma can develop from precursor lesions, including pancreatic intraepithelial neoplasia and intraductal papillary mucinous neoplasm (IPMN). Previous studies indicated that loss of *Acvr1b* accelerates the Kras-mediated development of papillary IPMN in the mouse pancreas; however, the cell type predominantly affected by these genetic changes remains unclear. **METHODS:** We investigated the contribution of cellular origin by inducing IPMN associated mutations (KRAS^{G12D} expression and *Acvr1b* loss) specifically in acinar (*Ptf1a^{CreER};Kras$^{LSL-G12D}$; Acvr1b$^{fl/fl}$* mice) or ductal (*Sox9CreER;Kras$^{LSL-G12D}$;Acvr1b$^{fl/fl}$* mice) cells in mice. We then performed magnetic resonance imaging and a thorough histopathologic analysis of their pancreatic tissues.

RESULTS: The loss of *Acvr1b* increased the development of pancreatic intraepithelial neoplasia and IPMN-like lesions when either acinar or ductal cells expressed a Kras mutation. Magnetic resonance imaging, immunohistochemistry, and histology revealed large IPMN-like lesions in these mice that exhibited features of flat, gastric epithelium. In addition, cyst formation in both mouse models was accompanied by chronic pancreatitis. Experimental acute pancreatitis accelerated the development of large mucinous cysts and pancreatic intraepithelial neoplasia when acinar, but not ductal, cells expressed mutant Kras and lost *Acvr1b*.

CONCLUSIONS: These findings indicate that loss of *Acvr1b* in the presence of the Kras oncogene promotes the development of large and small precancerous lesions from both ductal and acinar cells. However, the IPMN-like phenotype was not equivalent to that observed when these mutations were made in all pancreatic cells during development. Our study underscores the significance of the cellular context in the initiation and progression of precursor lesions from exocrine cells. *(Cell Mol Gastroenterol Hepatol 2024;18:101387; https://doi.org/10.1016/j.jcmgh.2024.101387)*

Pancreatic cancer initiation is associated with 3 main types of precancerous lesions: pancreatic intra-epithelial neoplasia (PanIN), intraductal papillary mucinous neoplasm (IPMN), and mucinous cystic neoplasm. PanIN and IPMN lesions are both mucinous and clinically they are largely distinguished by their size, with IPMN being a larger lesion type that can be detected by magnetic resonance imaging (MRI). Adult pancreatic ductal and acinar cells can both give rise to precancerous lesions in animal models[1-5] when mutations in *Kras*, the most commonly altered oncogene in pancreatic cancer, are present. However, most gene mutations and pathway alterations associated with pancreatic cancer have been studied in the context of pan-pancreatic genetic changes induced during pancreato-genesis.[6] Thus, how a particular gene affects the initiation and development of precancerous lesions and pancreatic cancer from either acinar or especially ductal cells is largely unknown.

Activin A receptor type 1B (ACVR1B) is a member of the transforming growth factor (TGF)-β superfamily of receptor serine/threonine kinase. Compared with the TGF-β and BMP pathways within the TGF-β superfamily, the understanding of activin signaling is not as comprehensive. Activins exert their effect by binding to either ACVR2A or ACVR2B (type II receptors), which prompts the recruitment of a type I receptor, such as ACVR1B. The activated receptor complex then activates SMAD2 and SMAD3, which forms a complex with SMAD4 and regulates gene transcription in the nucleus. Activin signaling plays a crucial role in several cellular processes, such as cell proliferation,[7-9] cell cycle arrest,[10] and apoptosis.[11,12] Dysregulation of activin signaling components has been implicated in several diseases, including cancer. Biallelic inactivation of *ACVR1B* has been reported in pancreatic cancer.[13,14] Mutations in *SMAD2/3/4*, which are downstream mediators of activin/TGF-β signaling, are also found in many cancers,[15] with 55% of pancreatic cancers having *SMAD4* loss.[16] Loss of *SMAD4* was primarily found in pancreatic ductal adenocarcinoma, but not the precancerous lesions. However, *Smad4* loss and *Acvr1b* loss in the pancreas using animal models is associated with the greater development of PanIN lesions, cystic pancreatic precursors, and pancreatic cancer development in the context of onco-genic Kras,[17-20] suggesting that the Activin arm of TGF-β superfamily can affect the initiation and development of precursor lesions.

In our previous studies, we showed that loss of *Acvr1b* in mouse pancreas using a mosaic *Pdx1Cre*[21] allele led to chronic pancreatitis around 9 months of age.[20] When these alleles were combined with the oncogenic *Kras^{LSL-G12D}* allele,[21] these mice developed cystic gastric and pancreatobiliary IPMN-like lesions beginning around 34 days of age, and numerous PanIN and pancreatic cancer.[20] These data suggested that loss of *Acvr1b* in the context of onco-genic Kras resulted in the induction of IPMN-like lesions. In *Pdx1Cre;Kras^{LSL-G12D};Acvr1b^{fl/fl}* (AKpdx1) mice gene mutations are targeted to early pancreatic progenitor cells, resulting in the genetic changes occurring in the developing endocrine, acinar, and ductal cell compartments. This made it unclear which specific cell types were contributing to the development of the IPMN-like lesions in AKpdx1 mice. To determine the consequence of *Acvr1b* loss specifically in acinar or ductal cells in the pancreas in the context of oncogenic Kras, we crossed *Kras^{LSL-G12D};Acvr1b^{fl/fl}* mice to mice expressing the CreER protein in an acinar- or ductal-cell-specific manner and examined the development of lesions by MRI and histopathology. We found that *Acvr1b* loss and activation of *Kras* in either the acinar or ductal cells results in chronic pancreatitis, increased formation of MRI-detectable mucinous cysts, and increased microscopic pre-cancerous lesions. Although some of these large cysts were mucinous, only AKpdx1 mice formed complex papillary IPMN-like lesions. This suggests that the phenotype in AKpdx1 mice is potentially the consequence of a complex interplay of events occurring during development of the pancreas in the context of these mutations or a result of mutations being present in large numbers of acinar and ductal cells.

Results

Acvr1b *Loss in Kras^{G12D}-Expressing Acinar or Ductal Cells Promotes Cyst Formation*

To determine the phenotypic consequences of *Acvr1b* loss in the context of Kras^{G12D} expression in postnatal ductal or acinar cells, we generated mouse models in which these genetic changes were induced in an acinar-cell-type- or ductal-cell-type-specific manner. Specifically, we used the tamoxifen-inducible *Ptf1a^{CreER}* allele[22] to induce Cre-dependent recombination of the *Kras^{LSL-G12D}*[21] and *Acvr1b^{flox}*[20] conditional alleles to express Kras^{G12D} and ablate *Acvr1b* expression (Figure 1A) in juvenile-aged acinar cells. By combining all of these alleles through cross-breeding, we generated *Ptf1a^{CreER};Kras^{LSL-G12D};Acvr1b^{fl/fl}* mice (AKpt) (Figure 1A). Mice lacking the *Acvr1b^{flox}* alleles were used as control animals (*Ptf1a^{CreER};Kras^{LSL-G12D}*) (Kpt). Using a similar approach, we combined the *Sox9CreER* allele[23,24] with the *Kras^{LSL-G12D}* and *Acvr1b^{flox}* conditional alleles to express Kras^{G12D} and ablate *Acvr1b* expression in postnatal ductal cells. This generated *Sox9CreER;Kras^{LSL-G12D};Acvr1b^{fl/fl}* (AKsox9) mice (Figure 1B). *Sox9CreER;Kras^{LSL-G12D}* mice (Ksox9) lacking the *Acvr1b* alleles were used as control animals. All mice were injected with tamoxifen at 3–4 weeks of age and then subsets of mice were subjected to MRI and survival studies, whereas others were collected at various time points for histologic analyses.
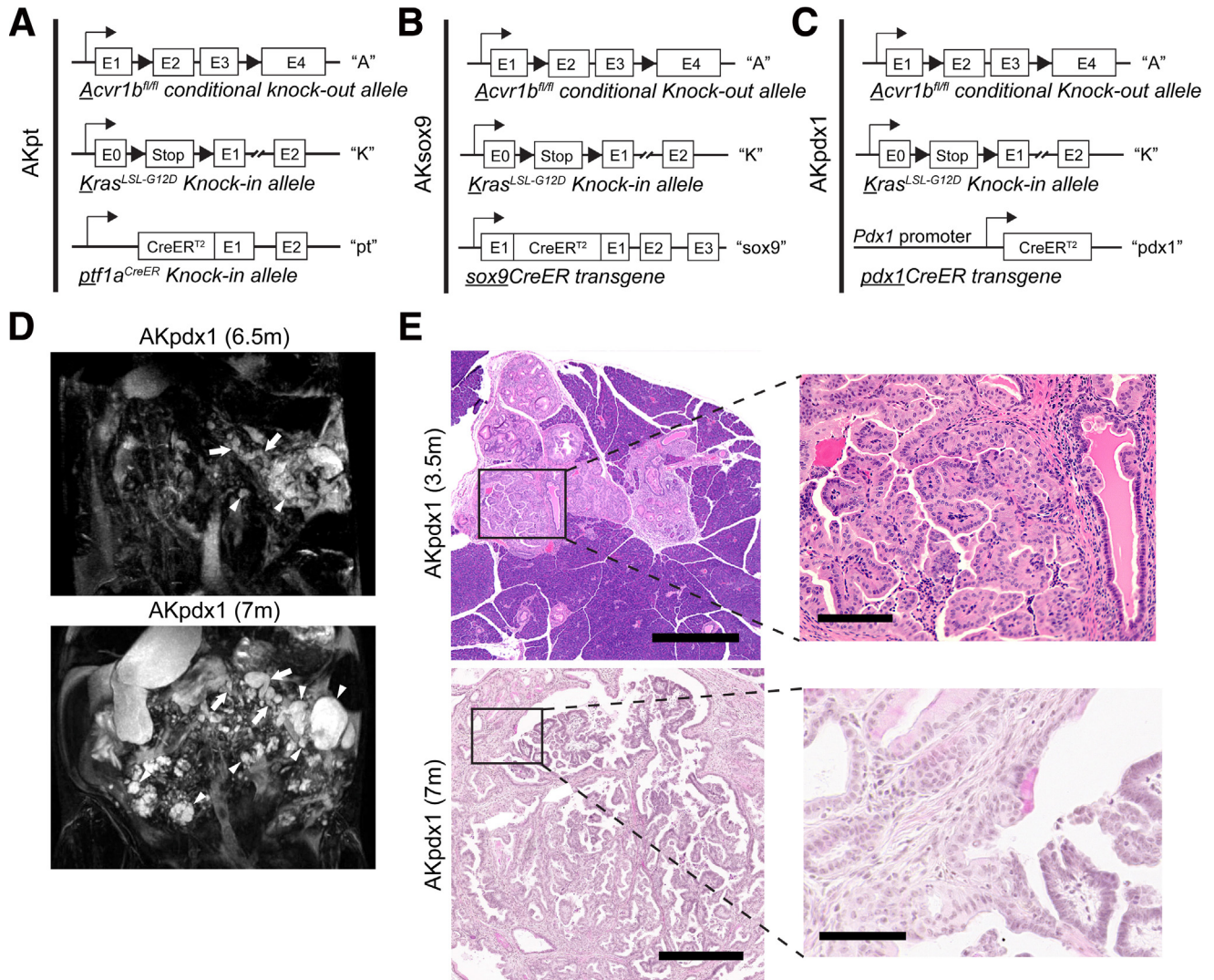
A

B

C

D AKpdx1 (6.5m)

E


Figure 1. *Acvr1b* loss in Kras^{G12D}-expressing acinar cells results in pancreatic cysts throughout the pancreas. (*A–C*) Schematic of the alleles in the *Ptf1a^{CreER};Kras$^{LSL-G12D}$;Acvr1b$^{fl/fl}$* (AKpt) mice (*A*), *Sox9CreER;Kras$^{LSL-G12D}$;Acvr1b$^{fl/fl}$* (AKsox9) mice (*B*), and *Pdx1Cre;Kras$^{LSL-G12D}$;Acvr1b$^{fl/fl}$* (AKpdx1) mice (*C*) used in this study. (*D*) Representative T2-weighted MRIs of the AKpdx1 mice (n = 4) at the age of 6.5 and 7 months (m) depicting multiple cystic lesions (*arrowheads*), and dilation of the main pancreatic duct (*arrows*). (*E*) Low (*left*) and high (*right*) magnification images of hematoxylin-eosin-stained sections from the pancreas of AKpdx1 mice at 3.5 or 7 months of age. Scale bars: 400 μm (*E*, *left*); 80 μm (*E*, *right*).

Survival studies with AKpt mice (n = 20) and AKsox9 mice (n = 5) found that AKpt mice had a median survival of 363 days (Supplementary Table 1). This survival time is shorter than the reported median survival of *Pdx1Cre;K-ras^{G12D}* mice (~400 days),[25] suggesting that *Acrv1b* loss in Kras^{G12D}-expressing acinar cells does reduce survival time in AKpt mice. Unlike AKpt mice, none of the AKsox9 mice reached humane end point by 17 months of age, which is consistent with previous studies showing that very few precancerous lesions are induced by oncogenic Kras^{G12D} expression in ductal cells.[1,2]

Our previous studies with AKpdx1 mice suggested that cystic lesions consistent with IPMN could form,[20] therefore we also monitored a subset of AKpt (n = 3) and AKsox9 (n = 11) mice with MRI and compared them with AKpdx1 mice (Figure 1*C*; n = 4). As expected, MRI showed that all

AKpdx1 mice had multiple cysts (Figure 1*D*), and main pancreatic duct dilation (Figure 1*D* and Supplementary Table 2). Consistent with our previous studies,[20] histologic analyses of these AKpdx1 mice confirmed the presence of complex arborizing papillary lesions affecting the main pancreatic duct (Figure 1*E*). In AKpt mice, 2 of 3 mice had multiple cysts detected by MRI (Figure 2*A*), but no main pancreatic duct dilation was observed in these 2 cases by 8 months of age (Figure 2*A* and Supplementary Table 2). Histologic analyses of these mice confirmed the presence of large cysts lined by a morphologically normal but inflamed ductal epithelium or a mucinous flat epithelium (Figure 2*C*). Importantly, in most AKpt mice at survival end point, almost the entire parenchyma was replaced with a mix of these cysts, PanIN, and other evidence of chronic pancreatitis (Figure 2*B* and *D*). There was also pancreatic cancer in
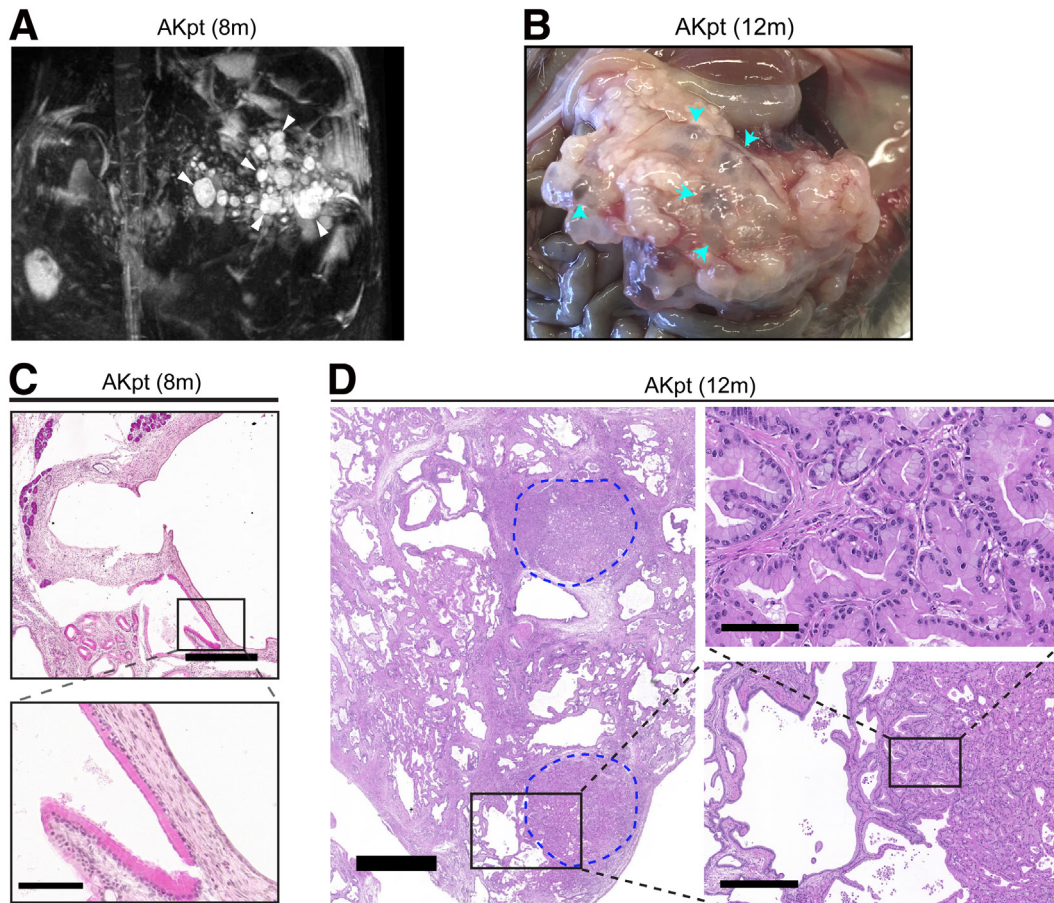
Figure 2. *Acvr1b* **loss and Kras activation in acinar cells is associated with multiple cysts and nodules of pancreatic cancer.** (*A*) Representative T2-weighted MRI of AKpt mice (n = 3) at the age of 8 months depicting multiple cystic lesions (*arrowheads*); no main pancreatic duct dilation was observed. (*B*) Representative gross anatomic photograph of the abdomen from AKpt mice (n = 13) at ∼12 months of age (m). Some of the numerous scattered pancreatic cysts are denoted with *blue arrowheads*. (*C*) Low- and high-magnification images of H&E-stained sections from *Ptf1a^{CreER};Kras^{LSL-G12D};Acvr1b^{fl/fl}* (AKpt) pancreata at 8 months of age. (*D*) H&E-stained section of the AKpt pancreas at 12 months of age showing multiple nodules of pancreatic cancer (outlined in *blue* and magnified in accompanying panels) among pancreatic cysts. Scale bars: 3 mm (*D*, *left*); 400 μm (*C*, *top* and *D*, *right bottom*); 100 μm (*D*, *right top*); 80 μm (*C*, *bottom*).

several AKpt mice at humane end point (Figure 2D). In sum, AKpt mice did form MRI-detectable mucinous cysts consistent with IPMN; however, the epithelium of these cysts was primarily flat and did not recapitulate the complex arborizing papilla that could be observed in AKpdx1 mice (Figure 1E).

MRI of AKsox9 mice found that 4 of 11 mice imaged developed detectable cysts and 1 of the 17-month-old mice had a large cyst accompanied by clear dilation of the main pancreatic duct (Figure 3A and Supplementary Table 2). By necropsy and histologically, many of the pancreata at 12 and 17 months of age were predominantly normal (Figure 3B) and the cysts that were present were predominantly lined by flat, reactive ductal cells (Figure 3C); however, some mice also had mucinous PanIN lesions (Figure 3D). Together these results indicated that *Acvr1b* loss and activation of Kras in ductal cells can result in ductal cysts that affect the main pancreatic duct. However, similar to AKpt mice, the

papillary nodules present in AKpdx1 mice were not present in AKsox9 mice.

Acvr1b Loss and Activation of Kras in Acinar Cells Promotes Formation of PanIN and IPMN-like Precancerous Lesions

To further characterize the events leading to cyst formation in AKpt mice, we histologically characterized AKpt mice at 3, 5, 7, and 9 months of age (Figure 4A). At 3 months of age, small areas of the AKpt pancreata had ductal metaplasia that replaced normal acinar cell area (acinar-to-ductal metaplasia [ADM]), and low-grade PanIN lesions (Figure 4A). In 5-month-old AKpt mice, ADM and immune cell infiltration was more prevalent (Figure 4A). In addition to low-grade PanIN, high-grade PanIN were also observed and these became more prevalent at 7 months of age (Figure 4A). In 9-month-old AKpt mice, large areas of the
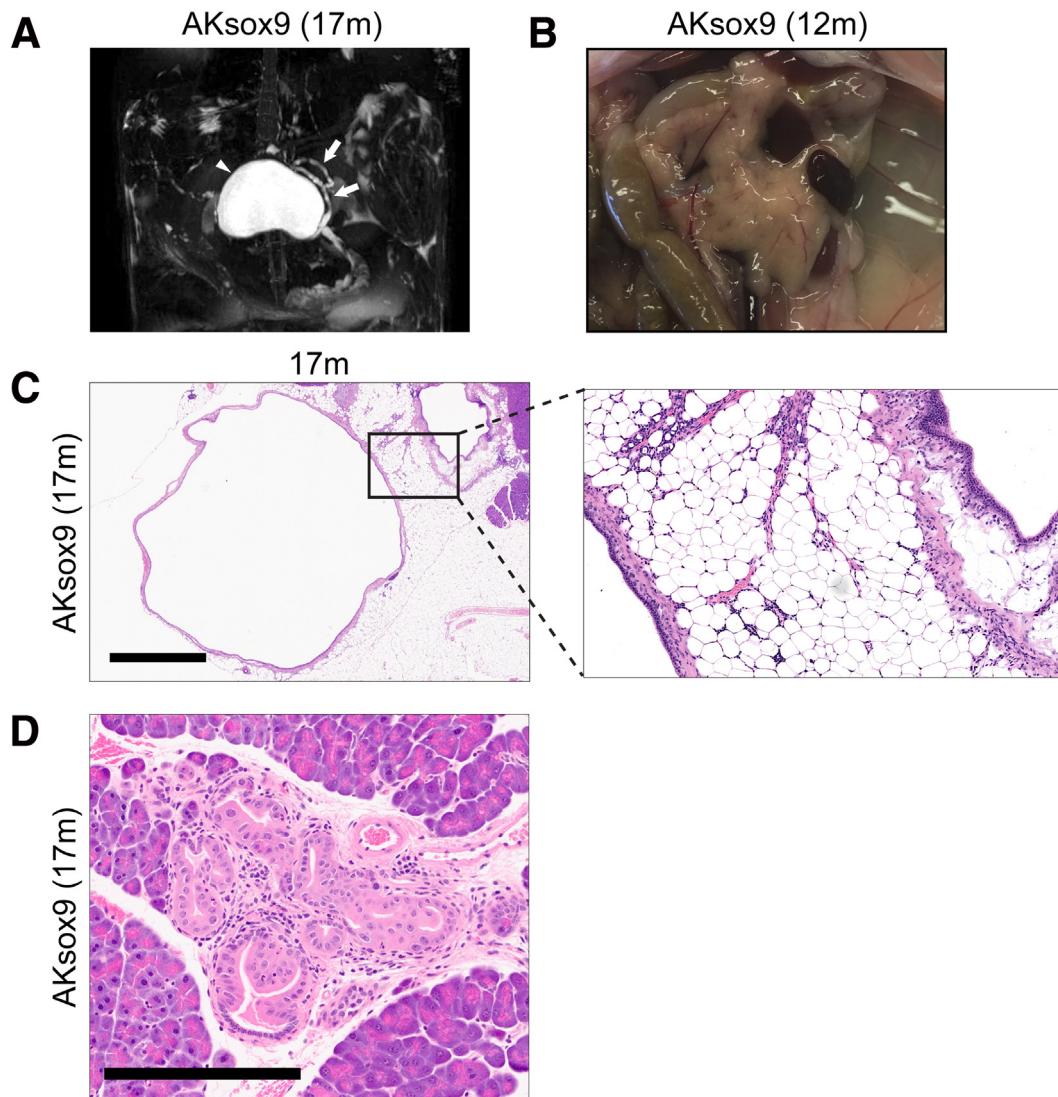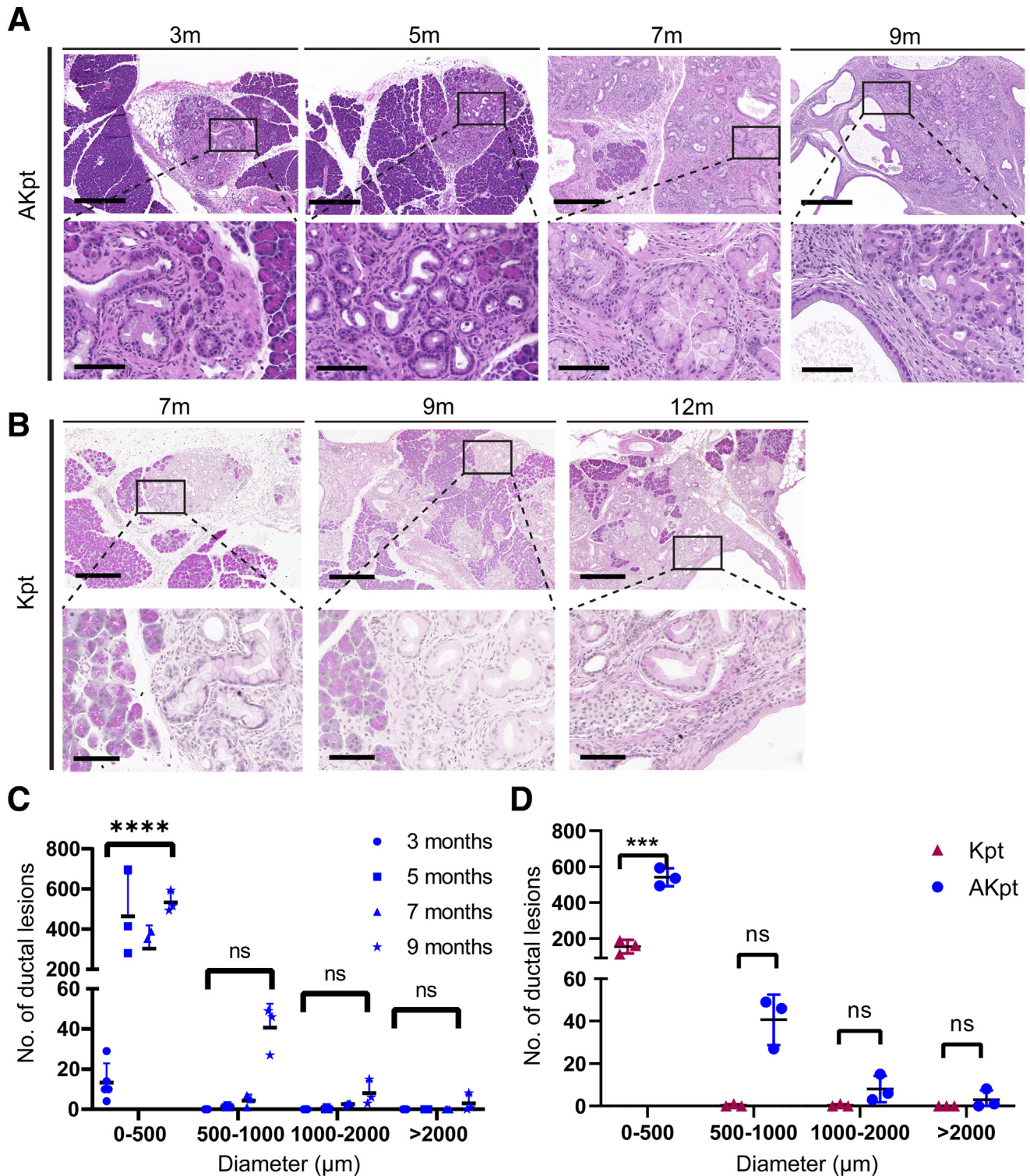
Figure 3. *Acvr1b* loss and activation of Kras in ductal cells is associated with dilation of the main pancreatic duct. (*A*) Representative MRI of *Sox9CreER;Kras^{LSL-G12D};Acvr1b^{fl/fl}* (AKsox9) mice (n = 5) at 17 months (m) of age depicting a large cyst (*arrowhead*), and dilation of the main pancreatic duct (*arrows*). (*B*) Representative gross anatomic photographs of the mouse abdomen from AKsox9 mouse at 12 months of age (n = 13). (*C* and *D*) H&E-stained sections of AKsox9 pancreata at 17 months of age depicting a large nonmucinous cyst and dilation of main pancreatic duct beside it (*C*, *left*) and fatty fibrosis between the 2 large ducts (*C*, *right*). (*D*) Example of a PanIN lesion found in AKsox9 mice at 17 months of age. Scale bars: 1.2 mm (*C*, *left*); 200 μm (*D*).

pancreas were displaced by large ductal cysts with reactive epithelium or mucinous characteristics (Figure 4*A*). One of 3 of the 7- and 9-month-old AKpt mice also developed pancreatic ductal adenocarcinoma (Figure 4*A*). In contrast, in 7-, 9-, and 12-month-old Kpt mice (Figure 4*B*), more normal parenchyma remained and the histologic changes consisted mostly of ADM or low-grade PanIN lesions, with very rare large cystic ducts. These results suggested that the combined effects of Kras mutation and *Acvr1b* loss in acinar cells resulted in formation of more precancerous lesions compared with Kras activation alone.

To more accurately quantify the histologic changes in the ductal lumens across AKpt pancreata collected at different ages (3, 5, 7, and 9 months), we measured the diameter and subcategorized abnormal ductal lesions into 4 size groups: 0–500 μm, 500–1000 μm, 1000–2000 μm, and >2000 μm (Figure 4*C* and Supplementary Table 3). At 3 months of age, all the ductal lesions were smaller than 500 μm (Figure 4*C*). However, from 5 months of age onward, we observed ductal structures larger than 500 μm, with an increase in the overall number of structures as the AKpt mice aged (Figure 4*C*). Additionally, we observed some abnormal ductal structures larger than 2000 μm at the age of 9 months (Figure 4*C*). Altogether, these findings suggested that the AKpt pancreata progressively become more cystic and this coincides with the progressive loss of normal parenchyma and widespread histologic evidence of chronic pancreatitis (Figure 4*A*). We further compared the number

Figure 4. *Acvr1b* loss and activation of Kras in acinar cells promotes initiation of pancreatic cysts with preneoplastic characteristics. (*A* and *B*) H&E-stained sections of *Ptf1a*^{CreER}*;Kras*$^{LSL-G12D}$*;Acvr1b*$^{fl/fl}$ (AKpt) pancreata at 3 (n = 5), 5 (n = 3), 7 (n = 3), and 9 months of age (n = 3) (*A*) or *Ptf1a*^{CreER}*;Kras*$^{LSL-G12D}$ (Kpt) mice at 7, 9, and 12 months of age (n = 3) (*B*). (*C* and *D*) Graphs depicting the number of the neoplastic structures at different size groups: 0–500 μm, 500–1000 μm, 1000–2000 μm, and >2000 μm in AKpt mice at 3 (n = 5), 5 (n = 3), 7 (n = 3), and 9 months of age (n = 3) (*C*) or in Kpt (n = 3) versus AKpt (n = 3) mice at the age of 9 months (*D*). ****P < .0001, ***P < .001, ns., not significant. Scale bars: *upper image* of set, 400 μm; *lower image* of set, 80 μm (*A* and *B*).

and size of ductal structures in AKpt (n = 3) and Kpt mice (n = 3) at the age of 9 months (Figure 4D and Supplementary Table 4). We found that AKpt mice had more ductal structures larger than 500 μm when compared with Kpt mice, and significantly more ductal lesions less than 500 μm (Figure 4D). These data suggested that loss of *Acvr1b* in Kras^{G12D}-expressing acinar cells results in increased preneoplastic formation overall and large cysts reminiscent of flat gastric IPMN-like lesions (>500 μm) form at later ages. Additionally, this increased lesion formation is accompanied by evidence of chronic pancreatitis.

Acvr1b *Loss and Activation of Kras Also Promotes Induction of Precancerous Lesions from Ductal Cells*

To further characterize the events associated with cyst formation in AKsox9 mice, we histologically characterized the pancreata of AKsox9 and Ksox9 mice at 5, 7, 9, or 12 months of age (Figures 5 and 6) and measured the diameter of the preneoplastic lesions in AKsox9 mice at 5, 7, 12, and 17 months of age (Figure 5B and Supplementary Table 5). Consistent with previous studies,[2] few PanIN lesions were observed in Ksox9 mice and only 2 of 6 mice examined had any PanIN at 5 or 9 months of age (Figure 6A and Supplementary Table 5). At 5 months of age, the AKsox9 pancreata were normal and no PanIN or pancreatitis was observed (Figure 5A and Supplementary Table 5). At 7, 12, and 17 months of age, preneoplastic lesions were observed in AKsox9 mice and the number of lesions per mouse increased with age (Figure 5A and B). These preneoplastic lesions were predominantly classified as PanIN; however, there were also larger mucinous cysts consistent with main duct IPMN of the flat, gastric type (Figure 5C and Supplementary Table 5). This suggests that loss of *Acvr1b* in ductal cells increases the formation of preneoplastic lesions from Kras^{G12D}-expressing ductal cells.

In addition to the observed precancerous lesions, we noted that there was evidence of chronic pancreatitis in multiple AKsox9 mice, including the formation of nodules of inflamed ducts, large cysts with reactive ductal epithelium, and fatty fibrosis surrounding the remnants of islets and ducts (Figures 3C, 5A, 5D, and Supplementary Table 5). This suggests that similar to *Pdx1Cre;Acvr1b*$^{fl/fl}$ mice,[20] loss of *Acvr1b* in ductal cells, at least in the context of KrasG12D expression, is associated with the development of chronic pancreatitis as the mice age.

Preneoplastic Lesions Induced by Acvr1b *Loss and Kras Activation have a Gastric Phenotype*

Low-grade PanIN lesions and mucinous cystic neoplasm lesions have a predominantly gastric type epithelium, whereas IPMN can be divided into 4 main epithelial phenotypes: gastric, intestinal, pancreatobiliary, and oncocytic type. Discrimination of these phenotypes is largely based on size; histologic and morphologic features; and the immunohistochemical expression pattern of MUC1, MUC2, and MUC5AC.[26–34] Because none of the lesions in AKpdx1, AKpt, or AKsox9 mice possessed the highly cellular stroma associated with mucinous cystic neoplasm lesions (Figures 1–5),[35] we focused here only on the histologic and immunohistochemical pattern of mucin expression. Histopathologic examination of IPMN-like lesions in AKpdx1 (3-month-old), AKpt (12-month-old), and AKsox9 (12-month-old) mice demonstrated that a small number of the cysts in AKpdx1 mice had a prominent proliferation of epithelial cells comprised of complex papillary projections (Figure 7). The papillary epithelium showed various grades of dysplasia from low grade to high grade. The preneoplastic cells in these AKpdx1 mice were composed of flat and papillary epithelium with abundant mucinous cytoplasm and were positive for alcian blue staining (Figure 7). Immunohistochemical staining for MUC1, MUC2, and MUC5AC (Figure 7) showed that these lesions expressed MUC1 and MUC5AC, but there was no expression of MUC2 (Figure 7). The mucinous IPMN-like cysts in AKpt and AKsox9 mice lacked the complex papillary projections and had a flat gastric epithelium (Figure 7). Consistent with this morphology, they were also positive for MUC1, MUC5AC, and alcian blue, but negative for MUC2. In sum, these findings indicate that the IPMN-like lesions in AKpdx1 mice are consistent with either gastric or pancreatobiliary IPMN, whereas those in the AKpt and AKsox9 mice have the features of gastric IPMN.

Caerulein Treatment Accelerates Formation of IPMN-like Lesions in AKpt Mice

Pancreatitis is known to accelerate the development of ADM/PanIN in the presence of oncogenic Kras and it is a risk factor for pancreatic cancer.[2,36–39] Because chronic pancreatitis was prominent in older AKpt mice and this was coincident with cyst formation, we next examined whether experimentally induced acute pancreatitis would also be sufficient to promote increased cyst formation in AKpt mice. Acute pancreatitis can be experimentally induced by treatment with supraphysiological levels of the cholecystokinin receptor agonist, caerulein.[40] To evaluate the impact of acute pancreatitis on the formation of PanIN and IPMN-like lesions following acinar cell-specific Kras activation with or without *Acvr1b* loss, we injected tamoxifen at 3–4 weeks of age and then induced caerulein-mediated acute pancreatitis in 6-week-old Kpt (n = 4) and AKpt mice (n = 4) and analyzed pancreatic tissue 21 days later (Figure 8A–C). Consistent with previous literature,[2] we confirmed that acute pancreatitis resulted in PanIN formation from oncogenic Kras-expressing acinar cells in Kpt mice by Day 21 (Figure 8B). In the AKpt mice, acute pancreatitis increased the replacement of acinar cells with ductal-like cells compared with Kpt mice, and more lesions with larger ductal lumens were observed (Figure 8B and C). To quantify the number of acinar cells in AKpt and Kpt mice, we performed immunohistochemistry to detect amylase in the pancreas of the caerulein-treated Kpt (n = 4) and AKpt mice (n = 4) and measured the amylase-positive pancreatic areas. The percentage of amylase-positive area in the AKpt mice was significantly lower than that of the Kpt mice ($P < .05$) (Figure 8D and Supplementary Table 6). We also
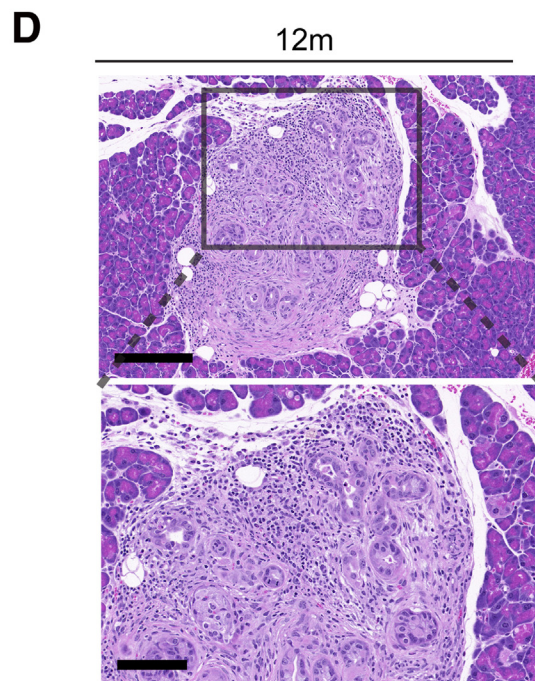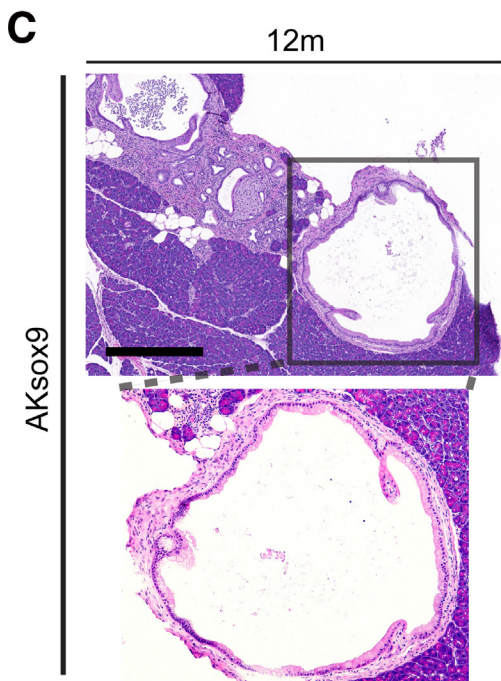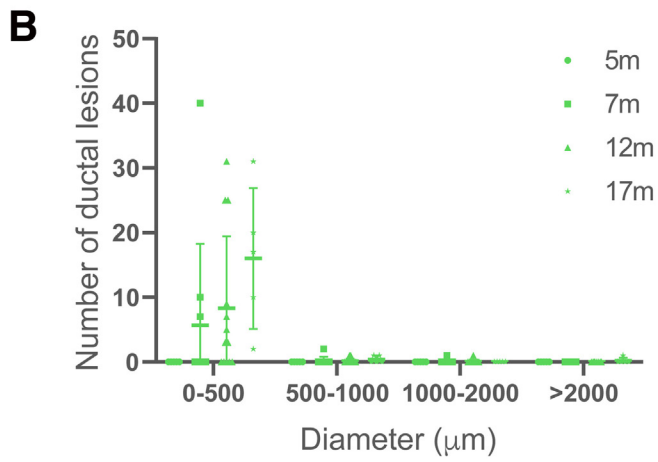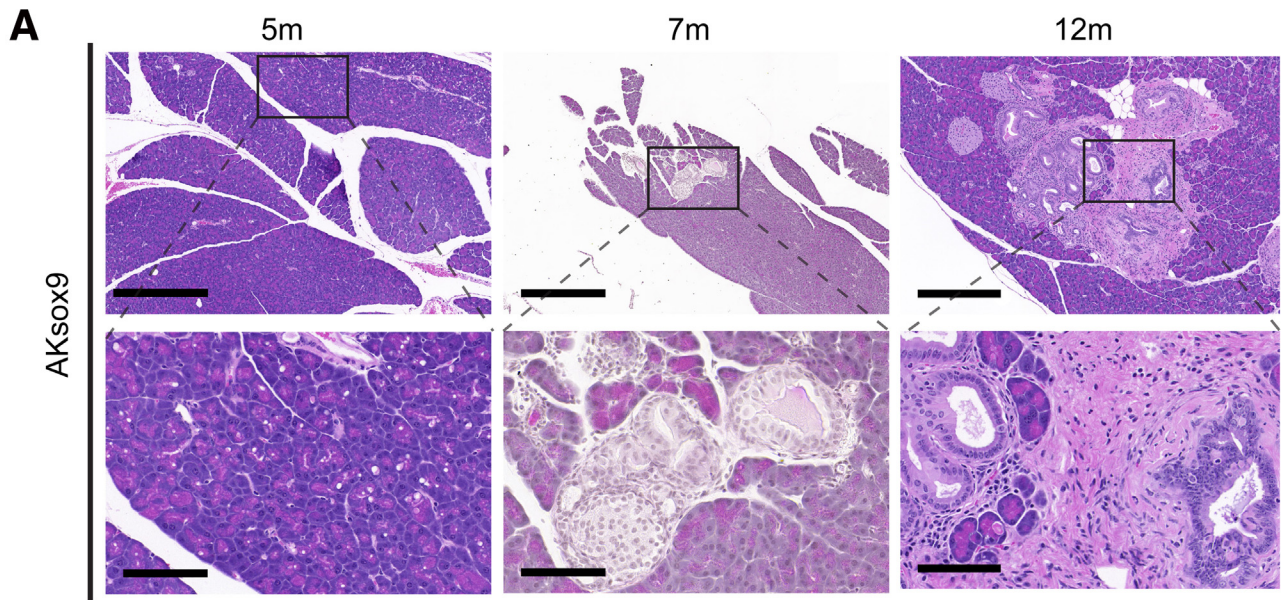
performed immunohistochemical staining for CK19 on Kpt (n = 4) and AKpt pancreata (n = 4) at Day 21 and quantified the CK19-positive areas. We found that the proportion of CK19-positive area in the AKpt mice was significantly higher than that of the Kpt mice (P < .05) (Figure 8E and Supplementary Table 6). Together these data indicate that loss of the activin receptor in AKpt mice resulted in a greater proportion of the parenchyma being affected 21 days after the induction of pancreatitis. We observed no difference in the relative amounts of CK19-positive ADM and PanIN lesions between genotypes; however, the epithelial lumens tended to be bigger on average with a larger number of IPMN-like cysts (lumen size >500 μm) in AKpt compared with Kpt mice (Figure 8C and 8F). In light of the absence of IPMN-like lesions in 3-month-old AKpt mice (Figure 4C and Supplementary Table 3), these results suggest that pancreatitis contributes to cyst development AKpt mice.

Precancerous Lesions Are Not Induced by Caerulein Treatment of AKsox9 Mice

IPMN and PanIN formation was also coincident with evidence of chronic pancreatitis in AKsox9 mice; therefore, we next examined how caerulein-mediated acute pancreatitis affects PanIN and IPMN formation from Kras[G12D]-expressing ductal cells with or without *Acvr1b* loss. To do this, we injected tamoxifen at 3–4 weeks of age and then induced caerulein-mediated acute pancreatitis in 6-week-old Ksox9 (n = 4–6) and AKsox9 mice (n = 3–4) and analyzed pancreatic tissue 2 or 21 days and 9 weeks later (Figure 9A). Similar amounts of inflammation and degranulation of the acinar cells was observed at 2 days after caerulein treatment in both genotypes, but we did not detect any PanINs in either Ksox9 or AKsox9 mice 21 days or 9 weeks after caerulein treatment (Figure 9B). These results suggested that short-term acute pancreatitis did not promote Kras[G12D]-expressing ductal cells to form preneoplastic lesions or cysts regardless of the *Acvr1b* genotype.

Discussion

In the Context of Oncogenic Kras, Embryonic Loss of Acvr1b Is Not Equivalent to Loss of Acvr1b Postnatally

Our previous studies suggested that IPMN resembling the gastric or pancreatobiliary subtypes were induced by oncogenic Kras and loss of *Acvr1b* in the pancreas.[20] Here, in this study, we found that inducing these same mutations in just the postnatal ductal or acinar cell populations did not result in IPMN with the complex arborizing papillae of pancreatobiliary IPMN. However, flat, mucinous, and large-lumened ductal cysts, consistent with gastric-type IPMN, and smaller lumen-sized PanIN, were observed, which is similar to the predominant phenotype found in AKpdx1 mice.[20] There are several possible reasons why the phenotype in AKpdx1 may not be recapitulated in the AKpt or AKsox9 mice. First, our previous studies suggested that loss of *Acvr1b* alone during pancreatogenesis did not affect pancreatic development because the minor pancreatitis phenotype was not observed until after 8 months of age.[20] However, AKpdx1 mice formed cysts as early as 1 month old;[20] this suggests that oncogenic Kras and loss of *Acvr1b* in combination might have affected some aspect of pancreatic development or the postnatal maturation of the pancreas and resulted in cyst and IPMN formation. Second, many pancreatic cell types are targeted when the *Pdx1Cre* allele is used. This can result in compound effects from both acinar and ductal cells being affected. Consistent with this possibility, the combined loss of *Acvr1b* and Kras activation was associated with chronic pancreatitis in AKsox9 mice (Figure 5D). Therefore, it is possible that pancreatitis that occurs as a result of loss of *Acvr1b* in Kras[G12D]-expressing ductal cells in AKpdx1 mice could have further exacerbated the phenotype of Kras[G12D]-expressing, *Acvr1b*-deleted acinar cells and vice versa. Lastly, as opposed to the AKsox9 and AKpt mouse models, islet cell types are also affected in AKpdx1 mice. Endocrine cells of the islet, particularly beta cells, are known to affect initiation of precancerous lesions by insulin/insulin receptor signaling in acinar cells.[41–43] Because Activin also affects insulin secretion from islets,[44,45] it is plausible that changes in Activin signaling in multiple cell types could result in a different phenotype in AKpdx1 mice compared with AKsox9 or AKpt mice.

Acvr1b Loss and Activation of Kras in Either the Acinar or Ductal Cell Lineages Promotes Formation of Precancerous Lesions

Our study demonstrates that loss of *Acvr1b* in juvenile ductal or acinar cells expressing Kras[G12D] results in the formation of more precancerous lesions compared with Kras[G12D] expression alone. In addition, some of the lesions in AKpt and AKsox9 mice become large cystic lesions with flat mucinous epithelium, consistent with gastric type IPMN. To date, most animal models of pancreatic cancer have focused on examining the effect of cancer-associated mutations in all pancreatic cells or by specifically examining the effect in acinar cells.[6] Thus, knowledge of how genetic changes affect tumorigenesis are largely based on the effects on all pancreatic cells in the context of an embryonic induction or on juvenile or adult acinar cells. Relatively recent studies have begun to identify how pancreatic

Figure 5. (*See previous page*). ***Acvr1b* loss and activation of Kras in ductal cells promotes formation of preneoplastic lesions and cysts.** (*A*) Representative images from H&E-stained sections of the *Sox9CreER;Kras[LSL-G12D];Acvr1b^{fl/fl}* (AKsox9) pancreata at 5 (n = 5), 7 (n = 10), and 12 months of age (n = 13). (*B*) Graph depicting the number of neoplastic structures in different size groups: 0–500 μm, 500–000 μm, 1000–2000 μm, and >2000 μm in the AKsox9 mice at 5 (n = 5), 9 (n = 10), 12 (n = 13), and 17 months of age (n = 5). (*C* and *D*) H&E-stained sections from AKsox9 mice at 12 months of age depicting a large preneoplastic cyst (*C*) and chronic pancreatitis (*D*). Scale bars: 480 μm (*C, upper image*); 300 μm (*C, lower image*); 200 μm (*D, upper image*, 100 μm (*A* and *D, lower image*).
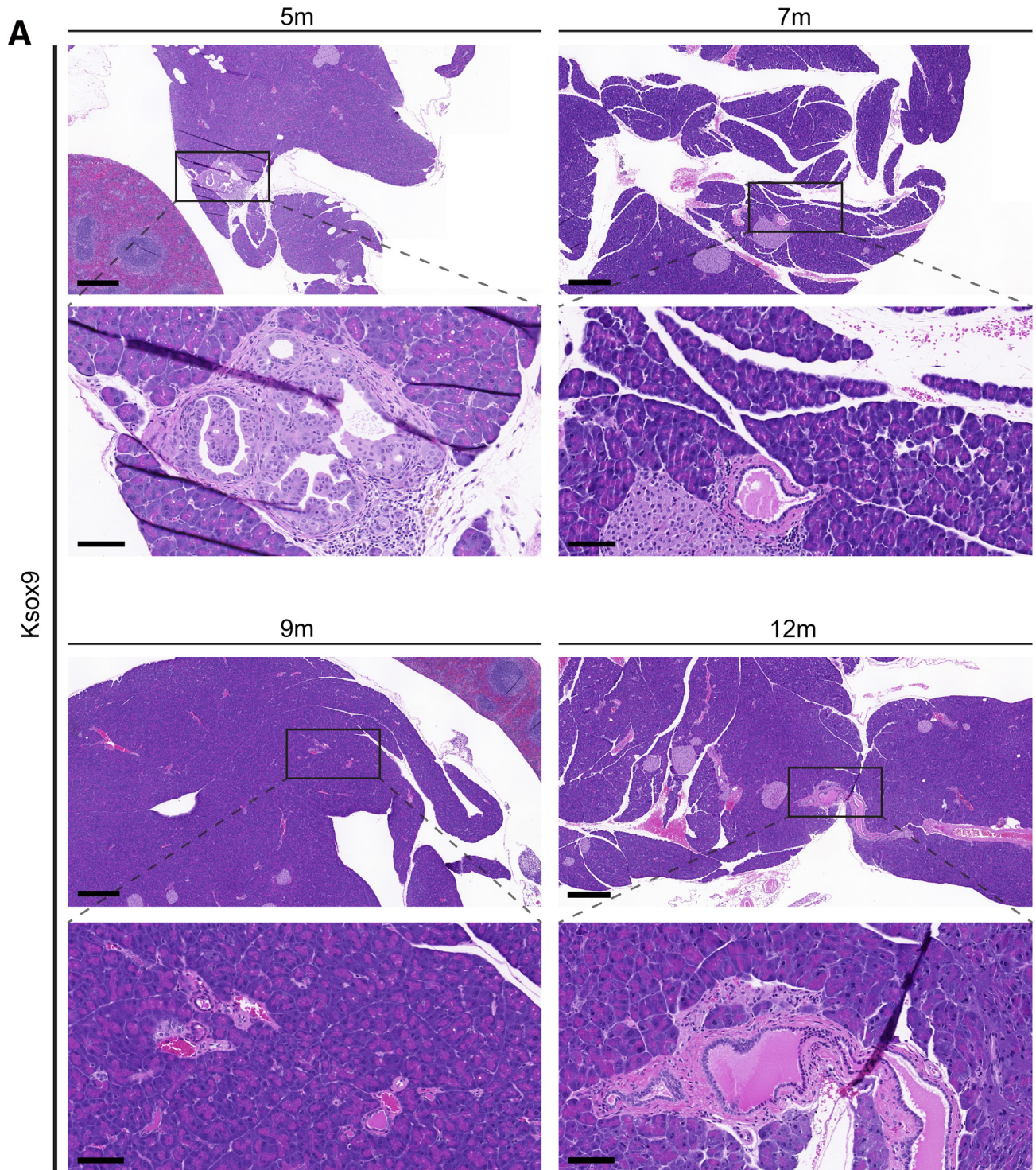
Figure 6. Ductal-cell-specific expression of oncogenic Kras results in few PanINs lesions. H&E-stained sections of the pancreas from *Sox9CreER;Kras*$^{LSL-G12D}$ (Ksox9) mice at 5, 7, 9, or 12 months of age. Out of the 6 Ksox9 mice analyzed only 1 mouse at 5 months old and 1 mouse at 9 months old had PanINs (Supplementary Table 4). Scale bars: *upper image* per set, 400 μm; *lower image* per set, 80 μm.

cancer–associated genetic changes affect ductal cells' contribution to pancreatic cancer in situ. The effects of the mutations studied, thus far, have shown that some of the mutations that affect tumorigenesis from ductal cells have little or opposite effects on acinar cells.[46–48] In our studies, we found that *Acvr1b* loss, likely through abrogation of Activin signaling, is one of the few pathways identified to date that promotes precancerous lesion formation from
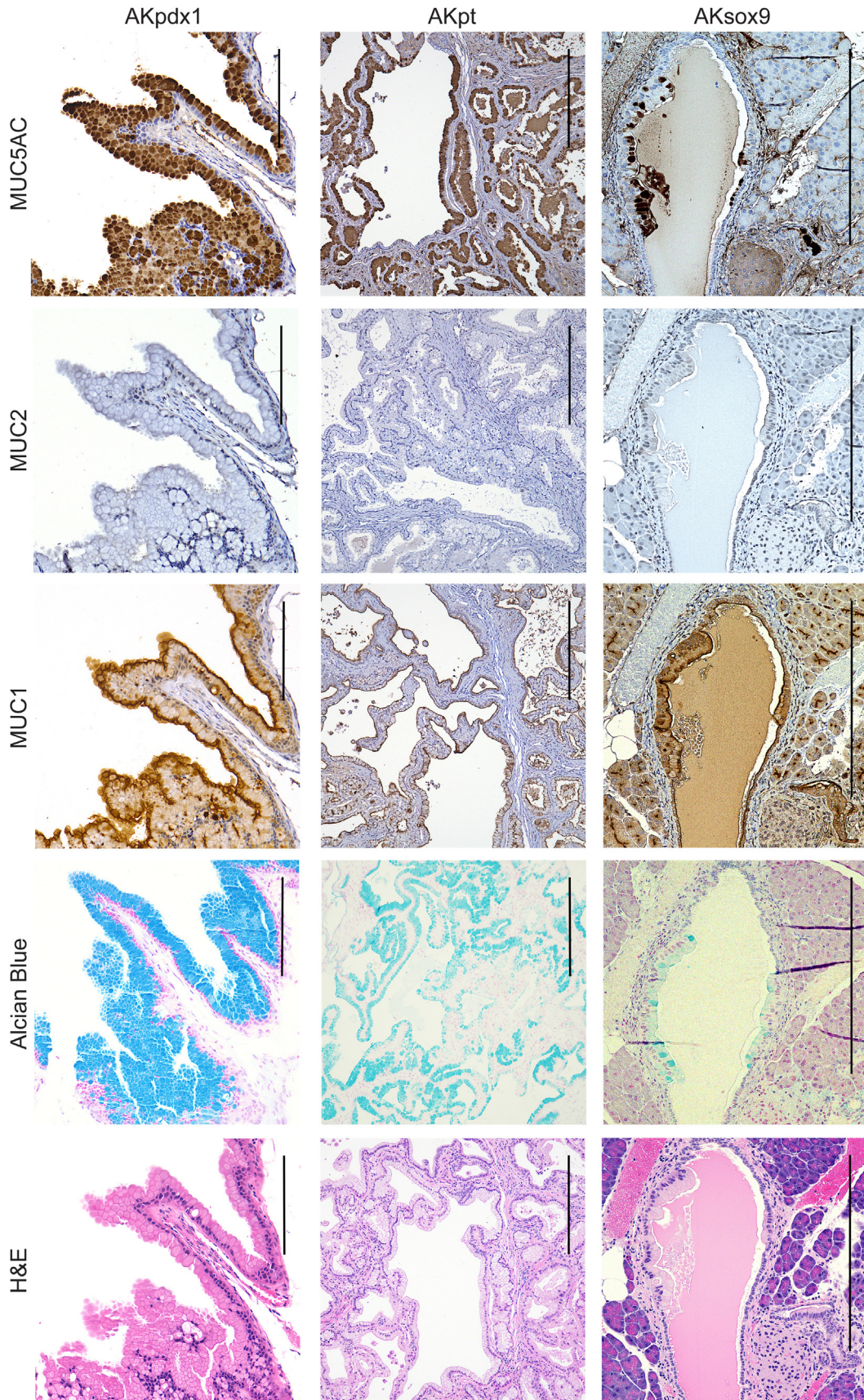
Figure 7. Morphologic and immunohistochemical analysis of the preneoplastic lesions in AKpdx1, Akpt, and AKsox9 mice. Representative images of H&E, alcian blue, MUC1, MUC2, and MUC5AC staining of the pancreas from mucinous large preneoplastic cysts in *Pdx1Cre;Kras^{LSL-G12D};Acvr1b^{fl/fl}* (AKpdx1), *Ptf1a^{CreER};Kras^{LSL-G12D};Acvr1b^{fl/fl}* (AKpt), or *Sox9CreER; Kras^{LSL-G12D};Acvr1b^{fl/fl}* (AKsox9) mice. Scale bars: 200 μm.
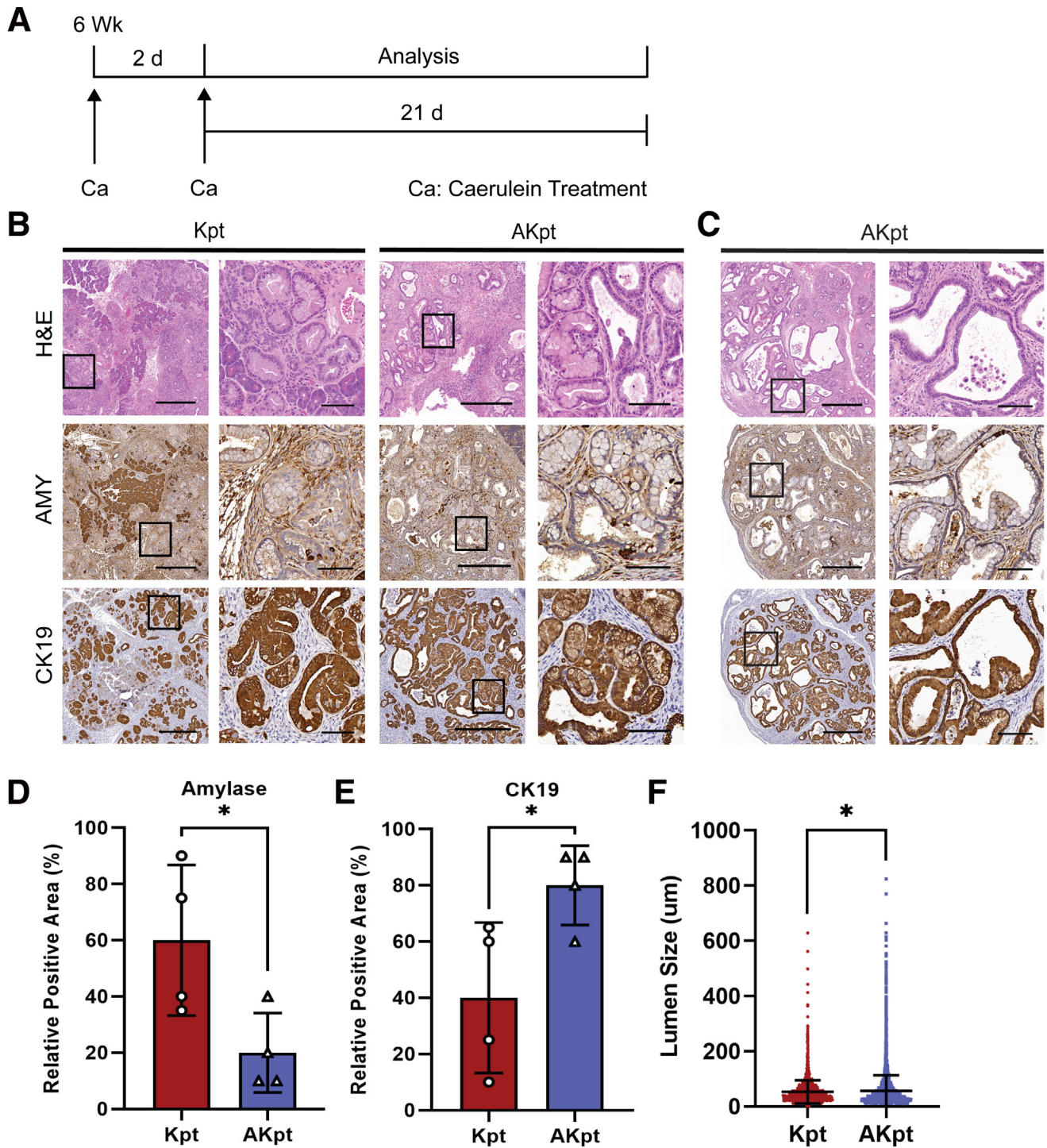
Figure 8. Caerulein treatment and *Acvr1b* loss promotes formation of IPMN-like lesions from Kras^{G12D}-expressing acinar cells. (*A*) Schematic of the caerulein treatment plan. At 6 weeks of age, *Ptf1a^{CreER};Kras$^{LSL-G12D}$* (Kpt) (n = 4) and *Ptf1a^{CreER};Kras$^{LSL-G12D}$;Acvr1b$^{fl/fl}$* (AKpt) (n = 4) mice were treated with 2 rounds of caerulein (Ca) injections on alternative days and analyzed 21 days later. (*B*) Representative images of H&E staining of the pancreata from Kpt and AKpt mice treated with caerulein at Day 21. Immunohistochemistry staining against amylase (AMY) or CK19 in Kpt or AKpt pancreata 21 days after caerulein treatment. (*C*) Representative images of H&E and immunohistochemistry staining of the larger ductal lumens found in pancreata from Kpt and AKpt mice at 21 days after caerulein treatment. (*D–F*) Quantification of the amylase-positive (*D*) or CK19-positive (*E*) pancreatic areas in the Kpt mice compared with the AKpt mice at 21 days after the caerulein treatment. (*F*) Quantification of lumen size across the entire section in Kpt or AKpt mice 21 days after caerulein treatment. *$P < .05$ by t-test (*D* and *E*) and nonparametric t-test (*F*). Scale bars: (*B* and *C*) *left image* of each set, 400 μm; *right image* of each set, 80 μm.

A

B
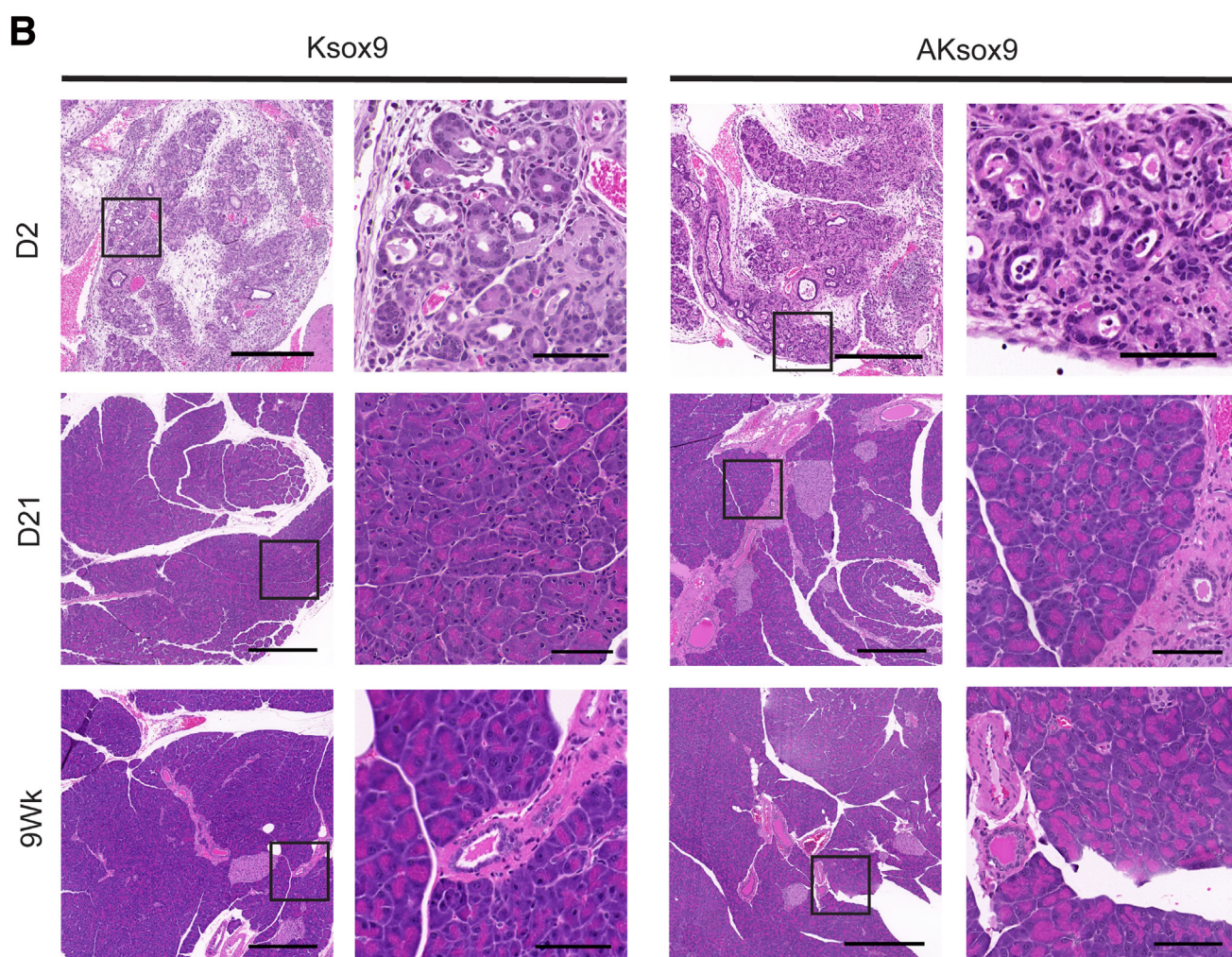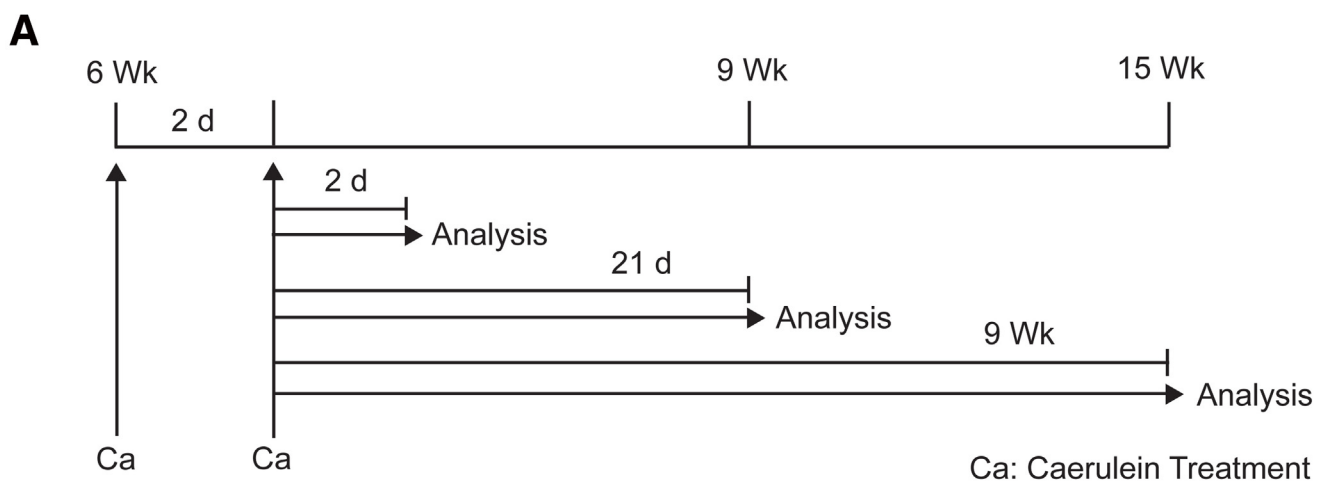
Figure 9. Kras-expressing ductal cells have a low propensity to form PanINs after chemically induced acute pancreatitis. (*A*) Schematic of the caerulein treatment plan. At 6 weeks of age, *Sox9CreER;Kras^LSL-G12D^;Acvr1b^fl/fl^* (AKsox9) (n = 4–6) and *Sox9CreER;Kras^LSL-G12D^* (Ksox9) (n = 3–4) mice were treated with 2 rounds of caerulein (Ca) injections on alternative days and analyzed at Day 2 or 21 (*D*), or 9 weeks (wk) later. (*B*) Representative images of H&E staining of the pancreas from Ksox9 or AKsox9 mice treated with caerulein, 2 or 21 days or 9 weeks posttreatment. Scale bars: (*B*) *left image* of each set, 400 μm; *right image* of each set, 80 μm.

both acinar and ductal cells expressing Kras[G12D]. However, the molecular mechanism by which this occurs is still unknown. It seems that rather than directly promoting precancerous lesion formation, Activin/Acvr1b signaling might affect the extent of inflammation in the pancreas that subsequently promotes formation of precancerous lesions. Previous studies have found that the expression of Activin increases in the epithelium during injury and Activin then acts on the macrophages to activate them.[49] Additionally, Activin-blocking antibody treatment of mice injected with caerulein reduced the severity of caerulein-induced pancreatitis in wild-type mice.[49] Thus, Activin signaling is clearly involved in pancreatitis, but further studies of ductal- or acinar-cell-specific Activin/Acvr1b signaling are needed to further understand how loss of *Acvr1b* affects the inflammatory signaling milieu in the pancreas in the presence or absence of Kras mutations.

Genetic Changes in Acinar and Ductal Cells can Contribute to Formation of IPMN-like Lesions

Our data suggest that loss of *Acvr1b* in Kras[G12D]-expressing ductal or acinar cells can lead to formation of large mucinous lesions akin to IPMN lesions, and cysts lined with nonmucinous epithelium. Previous studies have predominantly reported that only ductal cells can give rise to IPMN-like lesions, whereas the same mutations in acinar cells typically induce PanIN lesions or have no effect.[2,48,50,51] Rare instances of IPMN-like lesions occurring in the context of acinar-cell-specific mutations have been observed[52,53] (unpublished observation from[42]). Indeed, Flowers et al[53] used tdTomato lineage labeling with the same *Ptf1aCreER* allele used in our study to show that IPMN can be derived from Ptf1a^{+} cells. In our studies, it seems that effects of *Acvr1b* loss on cyst formation is not limited to either acinar or ductal cells; but caused by the increased effects of Kras[G12D] on the acinar cell population likely leads to a more consistent and robust phenotype in AKpt mice compared with AKsox9 mice. Specifically, in AKpt mice, more and/or earlier precancerous lesions form compared with Kpt mice. As a result, ductal metaplasia replaces most of the normal parenchyma and the ongoing inflammation from this metaplasia is associated with the formation of large nonmucinous and mucinous cysts, such as IPMN. This suggests that in the AKpt model inflammation is, in part, important for the cystic phenotype. This is likely similar to the role that *Elastase*-driven TGF-α expression has on IPMN formation in the context of Kras[G12D] expression in the entire pancreas.[52] In sum, experiments in mice suggest that it is possible for acinar cells to contribute to IPMN, but the applicability of these observations to human IPMN would be strengthened by future studies examining whether IPMN can originate from acinar cells when only a few of these cells sustain IPMN-associated mutations so that the large effects that occur after loss of the entire parenchymal function can be separated from the actions of the mutations in IPMN induction from acinar cells.

In AKsox9 mice, *Acvr1b*-loss-associated inflammation is also likely involved in the formation of main-duct IPMN and nonmucinous cysts. However, because *Kras[G12D]* mutations alone have very little effect on ductal cells,[1,2,54] this likely resulted in fewer precancerous lesions when compared with AKpt mice. Additionally, the large effects on the parenchyma in AKpt mice did not occur in AKsox9 mice. This makes interpreting the relationship between the inflammation and the induction precancerous lesions more straightforward. For example, it is easier to identify a mucinous lesion obstructing the main duct and conclude that it is downstream from the dilation and inflammation observed in an upstream area of the pancreas in these mouse models. In sum, inflammation likely has a large role in producing the conditions leading to formation of large cystic lesions that can be classified as IPMN from ductal cells. This duct-centric inflammation as a causative agent in IPMN formation seems consistent with location of main duct IPMN primarily within the preexisting ducts in patients.

Methods
Mouse Strains

LSL-Kras[G12D],[21] *Acvr1b^{fl/fl}*,[20] *Ptf1a[CreER]* (Jax No. 019378),[22] and *Sox9CreER*[23,24,46] mice have been described in detail previously. To induce recombination, 3- to 4-week-old mice were administered 3 subcutaneous injections of tamoxifen (Sigma Aldrich) in corn oil over 5 days (days 1, 3, and 5) at 5 mg/40 g body weight. *Ptf1a[CreER];Kras[LSL-G12D]* (Kpt) mice and *Sox9CreER;Kras[LSL-G12D]* (Ksox9) mice were used as control animals for *Ptf1a[CreER];Kras[LSL-G12D];Acvr1b^{fl/fl}* (AKpt) mice and *Sox9CreER;Kras[LSL-G12D];Acvr1b^{fl/fl}* (AKsox9) mice. No developmental effects were observed in these mice. All mice were housed in the Animal Care Facility at Columbia University Irving Medical Center, and the studies were conducted in compliance with the Columbia University Irving Medical Center Institutional Animal Care and Use Committee guidelines. Specifically, rapid weight loss in adjunct with body condition score less than 3 (Ullman-Cullere et al, Laboratory Animal Science, 1999), debilitating diarrhea, progressive dermatitis, rough hair coat, hunched posture, lethargy or persistent recumbency, coughing, labored breathing, nasal discharge, neurologic signs, bleeding from any orifice, self-induced trauma, shivering, a tumor burden of >10% body weight, ulceration of the tumor, or a mean tumor diameter >20 mm were considered a humane end point. If the animals lost more than 20% of their body weight, were cachectic, unable to obtain food or water, or their ocular and/or respiratory systems were compromised, they were euthanized.

Histologic and Immunolabeling Analyses

Murine tissues were fixed overnight in 10% neutral buffered formalin and embedded in paraffin. Routine hematoxylin-eosin staining was performed by the Histology Service Core Facility at Columbia University Irving Medical Center. KS and IW evaluated the histology of all sections and JLK, DFS, GHS, and Dr Wanglong Qiu (University Irvine Medical Center) provided a secondary analysis of key sections and all figures.

For histologic analyses, 1 section per mouse was examined in its entirety and the number of ductal lesions/lumens and their respective diameters were measured.

Immunohistochemistry was performed using unstained 5-μm sections derived from the formalin-fixed and paraffin-embedded blocks that were deparaffinized in xylene 3 times and rehydrated in ethanol 4 times. Heat-induced antigen retrieval was performed on all slides in Tris-EDTA buffer (0.5% Tween-20, citrate buffer, pH 6.8) in a steamer for 30 minutes. Slides were incubated with Dako peroxidase block buffer to block endogenous peroxidase activity. Primary antibody staining was performed at 4°C overnight. The secondary antibodies were detected with a 40-minute incubation with biotinylated universal secondary antibodies (Dako, Carpinteria, CA) and streptavidin–horseradish peroxidase. Hematoxylin was then used as a counterstain. Slides were dehydrated in ethanol then xylene and mounted with VectaMount permanent mounting medium (Vector Laboratories, Burlingame, CA). The following primary antibodies were used for immunohistochemistry: amylase (1:100, cat: sc-46657, Santa Cruz), CK19 (1:500, cat: ab52625, Abcam), MUC1 (1:100, #BS-1497R, Bioss Inc), MUC2 (SC-15334, Santa Cruz), and MUC5AC (#BS-7166R, Bioss Inc).

For quantification of the immunohistochemistry (CK19 and amylase), 1 section per mouse was examined in its entirety and the percentages of the CK19- or amylase-positive areas in each mouse were calculated by their proportions to the entire section.

For alcian blue staining, 5-μm sections were deparaffinized and rehydrated as in immunohistochemistry staining. Then slides were stained with alcian blue solution (1 g alcian blue in 100 mL 3% glacial acetic acid, pH 2.5) for 30 minutes at room temperature. Counterstaining with 0.1% nuclear fast red solution (0.1 g nuclear fast red and 5 g ammonium sulfate in 100 mL dH2O) was performed for 5 minutes. Slides were dehydrated and mounted.

Images were primarily captured using a 3-dimensional Histotech slide scanner and exported using the Aperio ImageScope program.

Caerulein Treatment

Acute pancreatitis was induced at 6 weeks of age in AKpt, Kpt, AKsox9, and Ksox9 mice by 2 sets of 6 hourly intraperitoneally caerulein injection (50 μg/kg diluted in saline; Sigma-Aldrich) separated by 24 hours. In this experiment, the final day of the caerulein/saline injection was considered Day 0,[2,36] and the pancreata were collected as indicated.

MRI Experiment

MRI data were obtained on a Bruker BioSpec 9.4T Magnetic Resonance Imager (Bruker Corp, Billerica, MA). The mice were anesthetized with 1%–2% isofluorane mixed with medical air via a nose cone. The concentration of the isoflurane was adjusted during the procedure to maintain the respiration rate in the range of 40–70 breaths/minute using a respiration pillow attached to a monitoring system (SA Instruments, Stony Brook, NY). Body temperature was maintained around 37°C using a flowing water heating pad. Low-resolution T1-weighted scout images were obtained initially. A rapid acquisition with relaxation enhancement sequence was used to acquire a high-resolution T2-weighted images with the following parameters: repetition time = 4873 ms, echo time = 60 ms, field of view = 34 × 34 mm, matrix size =256 × 256, slice thickness = 0.4 mm with 30 slices to cover the entire abdomen. Maximum intensity projection technique was used for the visualization of the cysts.

Statistical Analysis

P values were calculated using the 2-way analysis of variance with GraphPad Prism version 8.0.2. *P* values < .05 were determined to be significant.

Supplementary Material

Note: To access the supplementary material accompanying this article, go to the full text version at https://doi.org/10.1016/j.jcmgh.2024.101387.

References

1. Ray KC, Bell KM, Yan J, et al. Epithelial tissues have varying degrees of susceptibility to Kras(G12D)-initiated tumorigenesis in a mouse model. PLoS One 2011;6:e16786.
2. Kopp JL, Figura G von, Mayes E, et al. Identification of Sox9-dependent acinar-to-ductal reprogramming as the principal mechanism for initiation of pancreatic ductal adenocarcinoma. Cancer Cell 2012;22:737–750.
3. Habbe N, Shi G, Meguid RA, et al. Spontaneous induction of murine pancreatic intraepithelial neoplasia (mPanIN) by acinar cell targeting of oncogenic Kras in adult mice. Proc Natl Acad Sci 2008;105:18913–18918.
4. O J-PDL, Emerson LL, Goodman JL, et al. Notch and Kras reprogram pancreatic acinar cells to ductal intraepithelial neoplasia. Proc National Acad Sci 2008;105:18907–18912.
5. Friedlander SYG, Chu GC, Snyder EL, et al. Context-dependent transformation of adult pancreatic cells by oncogenic K-Ras. Cancer Cell 2009;16:379–389.
6. Xu Y, Liu J, Nipper M, et al. Ductal vs. acinar? Recent insights into identifying cell lineage of pancreatic ductal adenocarcinoma. Ann Pancreat Cancer 2019;2:11.
7. Burdette JE, Jeruss JS, Kurley SJ, et al. Activin A mediates growth inhibition and cell cycle arrest through Smads in human breast cancer cells. Cancer Res 2005;65:7968–7975.
8. Yamato K, Koseki T, Ohguchi M, et al. Activin A Induction of cell-cycle arrest involves modulation of cyclin D2 and p21CIP1/WAF1 in plasmacytic cells. Mol Endocrinol 1997;11:1044–1052.
9. Zauberman A, Oren M, Zipori D. Involvement of p21WAF1/Cip1, CDK4 and Rb in activin A mediated signaling leading to hepatoma cell growth inhibition. Oncogene 1997;15:1705–1711.

10. Togashi Y, Kogita A, Sakamoto H, et al. Activin signal promotes cancer progression and is involved in cachexia in a subset of pancreatic cancer. Cancer Lett 2015; 356:819–827.

11. Ying S, Zhang Z, Batres Y, et al. p53 is involved in the inhibition of cell proliferation mediated by activin A in cultured human prostate cancer LNCaP cells. Int J Oncol 1997;11:591–595.

12. Valderrama-Carvajal H, Cocolakis E, Lacerte A, et al. Activin/TGF-β induce apoptosis through Smad-dependent expression of the lipid phosphatase SHIP. Nat Cell Biol 2002;4:963–969.

13. Togashi Y, Sakamoto H, Hayashi H, et al. Homozygous deletion of the activin A receptor, type IB gene is associated with an aggressive cancer phenotype in pancreatic cancer. Mol Cancer 2014;13:126.

14. Su GH, Bansal R, Murphy KM, et al. ACVR1B (ALK4, activin receptor type 1B) gene mutations in pancreatic carcinoma. Proc Natl Acad Sci 2001;98:3254–3257.

15. Samanta D, Datta PK. Alterations in the Smad pathway in human cancers. Front Biosci 2012;17:1281.

16. Blackford A, Serrano OK, Wolfgang CL, et al. SMAD4 gene mutations are associated with poor prognosis in pancreatic cancer. Clin Cancer Res 2009;15:4674–4679.

17. Kojima K, Vickers SM, Adsay NV, et al. Inactivation of Smad4 accelerates Kras(G12D)-mediated pancreatic neoplasia. Cancer Res 2007;67:8121–8130.

18. Izeradjene K, Combs C, Best M, et al. Kras(G12D) and Smad4/Dpc4 haploinsufficiency cooperate to induce mucinous cystic neoplasms and invasive adenocarcinoma of the pancreas. Cancer Cell 2007;11:229–243.

19. Bardeesy N, Cheng K-H, Berger JH, et al. Smad4 is dispensable for normal pancreas development yet critical in progression and tumor biology of pancreas cancer. Genes Dev 2006;20:3130–3146.

20. Qiu W, Tang SM, Lee S, et al. Loss of activin receptor type 1B accelerates development of intraductal papillary mucinous neoplasms in mice with activated KRAS. Gastroenterology 2016;150:218–228.e12.

21. Hingorani SR, Petricoin EF, Maitra A, et al. Preinvasive and invasive ductal pancreatic cancer and its early detection in the mouse. Cancer Cell 2003;4:437–450.

22. Pan FC, Bankaitis ED, Boyer D, et al. Spatiotemporal patterns of multipotentiality in Ptf1a-expressing cells during pancreas organogenesis and injury-induced facultative restoration. Development 2013;140:751–764.

23. Font-Burgada J, Shalapour S, Ramaswamy S, et al. Hybrid periportal hepatocytes regenerate the injured liver without giving rise to cancer. Cell 2015;162:766–779.

24. Lee AYL, Dubois CL, Sarai K, et al. Cell of origin affects tumour development and phenotype in pancreatic ductal adenocarcinoma. Gut 2018;68:487.

25. Hingorani SR, Wang L, Multani AS, et al. Trp53R172H and KrasG12D cooperate to promote chromosomal instability and widely metastatic pancreatic ductal adenocarcinoma in mice. Cancer Cell 2005;7:469–483.

26. Adsay V, Mino-Kenudson M, Furukawa T, et al. Pathologic evaluation and reporting of intraductal papillary mucinous neoplasms of the pancreas and other tumoral intraepithelial neoplasms of pancreatobiliary tract: recommendations of Verona Consensus Meeting. Ann Surg 2016;263:162–177.

27. Basturk O, Hong S-M, Wood LD, et al. A revised classification system and recommendations from the Baltimore Consensus Meeting for Neoplastic Precursor Lesions in the Pancreas. Am J Surg Pathol 2015; 39:1730–1741.

28. Noë M, Brosens LAA. Gastric- and intestinal-type IPMN: two of a kind? Virchows Arch 2020;477:17–19.

29. Omori Y, Ono Y, Kobayashi T, et al. How does intestinal-type intraductal papillary mucinous neoplasm emerge? CDX2 plays a critical role in the process of intestinal differentiation and progression. Virchows Arch 2020; 477:21–31.

30. Adsay NV, Merati K, Andea A, et al. The dichotomy in the preinvasive neoplasia to invasive carcinoma sequence in the pancreas: differential expression of MUC1 and MUC2 supports the existence of two separate pathways of carcinogenesis. Mod Pathol 2002;15: 1087–1095.

31. Adsay NV, Merati K, Basturk O, et al. Pathologically and biologically distinct types of epithelium in intraductal papillary mucinous neoplasms: delineation of an "intestinal" pathway of carcinogenesis in the pancreas. Am J Surg Pathol 2004;28:839–848.

32. Ban S, Naitoh Y, Ogawa F, et al. Intraductal papillary mucinous neoplasm (IPMN) of the gastric-type with focal nodular growth of the arborizing papillae: a case of high-grade transformation of the gastric-type IPMN. Virchows Arch 2006;449:112–116.

33. Ban S, Naitoh Y, Mino-Kenudson M, et al. Intraductal papillary mucinous neoplasm (IPMN) of the pancreas: its histopathologic difference between 2 major types. Am J Surg Pathol 2006;30:1561–1569.

34. Taki K, Ohmuraya M, Tanji E, et al. GNASR201H and KrasG12D cooperate to promote murine pancreatic tumorigenesis recapitulating human intraductal papillary mucinous neoplasm. Oncogene 2016;35: 2407–2412.

35. Yonezawa S, Higashi M, Yamada N, et al. Precursor lesions of pancreatic cancer. Gut Liver 2008;2:137–154.

36. Morris JP, Cano DA, Sekine S, et al. Beta-catenin blocks Kras-dependent reprogramming of acini into pancreatic cancer precursor lesions in mice. J Clin Invest 2010; 120:508–520.

37. Guerra C, Schuhmacher AJ, Cañamero M, et al. Chronic pancreatitis is essential for induction of pancreatic ductal adenocarcinoma by K-Ras oncogenes in adult mice. Cancer Cell 2007;11:291–302.

38. Lowenfels AB, Maisonneuve P, Cavallini G, et al. Pancreatitis and the risk of pancreatic cancer. N Engl J Med 1993;328:1433–1437.

39. Lowenfels AB, Maisonneuve P, Dimagno EP, et al. Hereditary pancreatitis and the risk of pancreatic cancer. International Hereditary Pancreatitis Study Group. J Natl Cancer Inst 1997;89:442–446.

40. Magaña-Gómez J, López-Cervantes G, Goel S. Caerulin-induced pancreatitis in rats: histological and genetic expression changes from acute phase to recuperation. World J Gastroenterol 2006;12:3999–4003.

41. Zhang AMY, Chu KH, Daly BF, et al. Effects of hyperinsulinemia on pancreatic cancer development and the immune microenvironment revealed through single-cell transcriptomics. Cancer Metab 2022;10:5.

42. Zhang AMY, Magrill J, Winter TJJ de, et al. Endogenous hyperinsulinemia contributes to pancreatic cancer development. Cell Metab 2019;30:403–404.

43. Zhang AMY, Xia YH, Lin JSH, et al. Hyperinsulinemia acts via acinar insulin receptors to initiate pancreatic cancer by increasing digestive enzyme production and inflammation. Cell Metab 2023;35:2119–2135.e5.

44. Zhang Y-Q, Cleary MM, Si Y, et al. Inhibition of activin signaling induces pancreatic epithelial cell expansion and diminishes terminal differentiation of pancreatic β-cells. Diabetes 2004;53:2024–2033.

45. Florio P, Luisi S, Marchetti P, et al. Activin A stimulates insulin secretion in cultured human pancreatic islets. J Endocrinol Investig 2000;23:231–234.

46. Kopp JL, Dubois CL, Schaeffer DF, et al. Loss of Pten and activation of Kras synergistically induce formation of intraductal papillary mucinous neoplasia from pancreatic ductal cells in mice. Gastroenterology 2018;154:1509–1523.e5.

47. Roy N, Malik S, Villanueva KE, et al. Brg1 promotes both tumor-suppressive and oncogenic activities at distinct stages of pancreatic cancer formation. Genes Dev 2015;29:658–671.

48. Figura G von, Fukuda A, Roy N, et al. The chromatin regulator Brg1 suppresses formation of intraductal papillary mucinous neoplasm and pancreatic ductal adenocarcinoma. Nature Cell Biol 2014;16:255–267.

49. Thomas AL, Castellanos K, Mancinelli G, et al. Activin A modulates inflammation in acute pancreatitis and strongly predicts severe disease independent of body mass index. Clin Transl Gastroenterol 2020;11:e00152.

50. Kimura Y, Fukuda A, Ogawa S, et al. ARID1A maintains differentiation of pancreatic ductal cells and inhibits development of pancreatic ductal adenocarcinoma in mice. Gastroenterology 2018;155:194–209.e2.

51. Collet L, Ghurburrun E, Meyers N, et al. Kras and Lkb1 mutations synergistically induce intraductal papillary mucinous neoplasm derived from pancreatic duct cells. Gut 2020;69:704.

52. Siveke JT, Einwächter H, Sipos B, et al. Concomitant pancreatic activation of Kras(G12D) and Tgfa results in cystic papillary neoplasms reminiscent of human IPMN. Cancer Cell 2007;12:266–279.

53. Flowers BM, Xu H, Mulligan AS, et al. Cell of origin influences pancreatic cancer subtype. Cancer Discov 2021;11:660–677.

54. Bailey JM, Hendley AM, Lafaro KJ, et al. p53 mutations cooperate with oncogenic Kras to promote adenocarcinoma from pancreatic ductal cells. Oncogene 2016;35:4282–4288.

CRediT Authorship Contributions
Kiyoshi Saeki (Conceptualization: Equal; Formal analysis: Lead; Investigation: Lead; Methodology: Lead; Validation: Lead; Writing – original draft: Lead)
Ian S. Wood, MD (Formal analysis: Supporting; Validation: Supporting; Writing – review & editing: Supporting)
Wei Chuan Kevin Wang, BS (Investigation: Supporting; Methodology: Supporting; Writing – review & editing: Supporting)
Shilpa Patil (Writing – review & editing: Equal)
Yanping Sun (Data curation: Supporting; Methodology: Supporting)
David F. Schaeffer, MD (Formal analysis: Supporting; Investigation: Supporting)
Gloria H. Su (Conceptualization: Lead; Funding acquisition: Lead; Supervision: Lead; Writing – original draft: Equal; Writing – review & editing: Equal)
Janel L. Kopp (Funding acquisition: Equal; Supervision: Equal; Writing – review & editing: Lead)

Conflicts of interest
The authors disclose no conflicts.